

Bo Wang · Min-chuan Zhan · De-chun Zhu ·
Wei Liu · Chu-sheng Chen

Oxygen permeation and stability of $Zr_{0.8}Y_{0.2}O_{1.9}$ – $La_{0.8}Sr_{0.2}CrO_{3-\delta}$ dual-phase composite

Received: 17 January 2006 / Accepted: 26 January 2006 / Published online: 8 March 2006
© Springer-Verlag 2006

Abstract A tubular membrane made of $Zr_{0.8}Y_{0.2}O_{1.9}$ (60 vol%) and $La_{0.8}Sr_{0.2}CrO_{3-\delta}$ was prepared by a standard ceramic process. Oxygen permeation through the membrane tube was examined by exposing its outer shell to air and sweeping its inner wall with pure helium or CO balanced with helium. An oxygen flux of 9.2×10^{-9} mol $cm^{-2} s^{-1}$ was measured at 950°C under air/He gradient, and a larger flux of 3.2×10^{-8} mol $cm^{-2} s^{-1}$ at 930°C under air/CO gradient. The membrane tube was found to exhibit excellent stability under highly reducing atmosphere and elevated temperatures. The oxygen permeation rate is likely to be increased through the modification of the surface and reduction of the membrane thickness.

Keywords Membrane · Composites · Oxygen permeation

Introduction

Dense membranes made of materials that can conduct both oxygen ions and electrons allow oxygen to permeate in the presence of oxygen partial pressure difference. The most investigated dense membranes are those of oxygen-deficient transition metal oxides of $ABO_{3-\delta}$ perovskite structure, in which oxygen ions are transported via the jumping of oxygen vacancies while electrons (holes) are conducted along the B–O–B networks in the oxides. A typical example of perovskite oxygen-permeable material is $La_{1-x}Sr_xCo_{1-y}Fe_yO_{3-\delta}$ [1].

The dense oxygen-permeable membrane may find applications in oxygen separation from air and in manip-

ulation of oxygen-consuming industrial chemical process. For example, the membrane-based reactor promises to significantly reduce the cost of conversion of methane to syngas [2, 3], an intermediate for production of liquid fuels, hydrogen, and other value-added chemicals. For such an application, the membrane is required to possess both high permeability and sufficient chemical and structural stabilities under stringent operation conditions. It has been found difficult for a single-phase material to meet all these requirements; improvement in one aspect of the material is often at the expense of the other aspect. One possible way round this problem is to use dual-phase composites as the membrane, in which oxygen ions and electrons transport through respective phases. A number of dual-phase composites have been examined [4–8]. But, due to the use of noble metals as an electronic conductor, most of these composite membranes are not promising for practical application.

Yttrium-stabilized zirconia and doped lanthanum chromite have long been used as the respective oxygen ionic conductor and electronic conductor in solid oxide fuel cells. Both materials exhibit excellent stability under stringent conditions with one side exposed to air and highly reducing fuel at elevated temperature. Therefore, it is reasonable to expect that composites made of these two oxides be permeable to oxygen and stable under stringent operation conditions. In this work, composite of $Zr_{0.8}Y_{0.2}O_{1.9}$ (60 vol%) – $La_{0.8}Sr_{0.2}CrO_{3-\delta}$ was prepared, and its oxygen permeability and stability were examined.

Experimental

$Zr_{0.8}Y_{0.2}O_{1.9}$ (denoted YSZ) powder was prepared using a coprecipitation method, and $La_{0.8}Sr_{0.2}CrO_{3-\delta}$ (denoted LSC) powder was prepared using a solid-state reaction method. YSZ and LSC powders with a volume ratio of 60:40 were thoroughly mixed by ball milling, and then were isostatically pressed into a tube under a pressure of 300 MPa, followed by sintering at 1,550°C for 10 h in air.

B. Wang · M.-c. Zhan · D.-c. Zhu · W. Liu · C.-s. Chen (✉)
Laboratory of Advanced Functional Materials and Devices,
Department of Materials Science and Engineering,
University of Science and Technology of China,
Hefei, Anhui 230026, People's Republic of China
e-mail: ccs@ustc.edu.cn
Tel.: +86-551-3602940
Fax: +86-551-3601592

The phase composition of the sintered tube was analyzed by XRD (Rigaku D/Max- γ A), and its surface morphology was examined by SEM (JEOL JSM-6700F). The density of the tube was determined using the Archimedes method.

The experimental setup for oxygen permeation measurements is schematically shown in Fig. 1. A sintered tube (inside diameter 0.65 cm, wall thickness 1.23 mm, length 1.32 cm, inner wall surface area 2.7 cm²) was sealed between two dense alumina tubes using Pyrex glass rings at 1,000°C (Before sealing, the outer shell and two ends, of the tube were polished.). And to ensure the gas tightness, a pressure was loaded vertically by a spring attached to the upper alumina tube. To establish the oxygen partial pressure difference required for oxygen permeation, the outer shell of the tube was exposed to the ambient air, and its inner wall was swept with a gas stream of helium or helium-diluted CO (volume ratio of CO to helium 20:80) at a rate of 30 cm³ min⁻¹. The composition of the effluent gas was analyzed by an online gas chromatography (Shimadzu GC-14C). The amount of oxygen that mechanically leaked from the airside of the membrane was subtracted from the total oxygen flux using the method described in [9]. And the leakage was below 1% in most of cases.

Results and discussion

Phase composition and microstructure

The sintered tube has a relative density over 98%. SEM observation (Fig. 2a) also confirms that the tube has been well densified after sintering at 1,550°C. Examination of XRD patterns shows that the sintered sample consists of

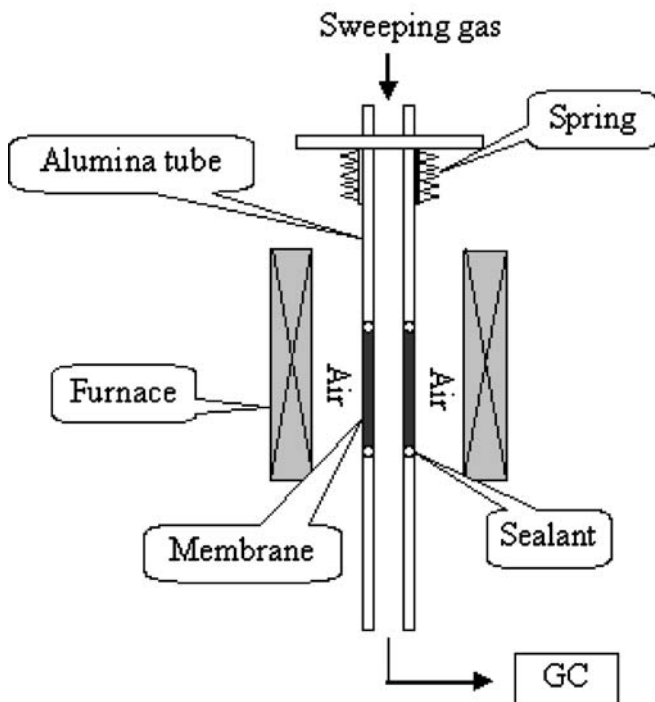


Fig. 1 Experimental setup for oxygen permeation

YSZ and LSC phases. Apparently, no significant reaction between YSZ and LSC oxides has occurred during high-temperature sintering, for all the XRD peaks in Fig. 3 can be assigned to either YSZ or LSC oxide. Besides, the good chemical stability of the two constituent oxides in the composite, both phases possess good mechanical compatibility, as their thermal expansion coefficients are close [10].

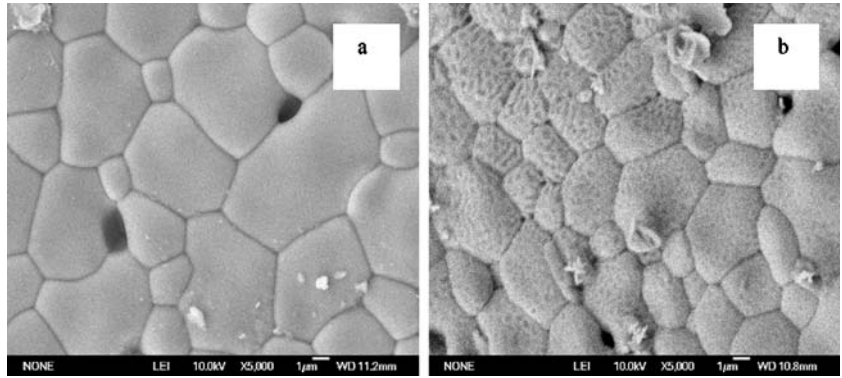
Oxygen permeation

Oxygen permeation through the as-prepared dual-phase composite tube was brought about at elevated temperatures by exposing the outer shell of tube to the ambient air and sweeping the inner wall with pure helium or helium-diluted CO. An oxygen permeation flux of 9.2×10^{-9} mol cm⁻² s⁻¹ was measured at 950°C under the air/He gradient. And when the sweeping gas was changed from helium to highly reducing CO, a much larger flux of 3.2×10^{-8} mol cm⁻² s⁻¹ was obtained (at 930°C). This is because in the latter case, the permeated oxygen readily reacted with highly reducing CO, resulting in a much lower oxygen partial pressure and, thus, a much larger driving force for oxygen permeation.

Figure 4a shows the Arrhenius plots of oxygen permeation flux under air/He and air/CO gradient. For comparison, oxygen permeance, defined as permeation flux normalized to the driving force, is presented in Fig. 4b. Note that a dual-phase composite membrane-based oxygen permeation cell is essentially an internally short-circuited electrochemical cell; thus, the driving force for oxygen permeation can be expressed as $E = \frac{RT}{4F} \ln \frac{p_{O_2}(h)}{p_{O_2}(l)}$, where F is the Faraday constant, $p_{O_2}(h)$ and $p_{O_2}(l)$ are the oxygen partial pressure at feed and permeate side, respectively [6]. From Fig. 4, it can be seen that the oxygen permeation flux under the air/He gradient is always lower than that under the air/CO gradient, whereas for the permeance crossover occurs. The temperature dependence of oxygen permeation is different for the two gradients. The associated activation energies for the measured oxygen permeation flux are 141 and 73 kJ mol⁻¹ for respective air/He and air/CO gradients, and the corresponding activation energies for the oxygen permeance are 147 and 84 kJ mol⁻¹, respectively.

The difference in permeance as well as the activation energy between the air/He and air/CO gradients is an indication that the rate-limiting step is different for the two gradients. It is known that oxygen permeation through the membrane consists of exchange of oxygen at the surfaces of the membrane and transport of oxide ions and electrons in the bulk of the membrane. It has been established that when the overall oxygen permeation process is limited by the bulk transport, the permeance is related to the ambipolar conductivity σ_{amb} according to $F_{O_2} = \frac{\sigma_{amb}}{4FL}$, where $\sigma_{amb} = \frac{\sigma_i \sigma_e}{\sigma_i + \sigma_e}$, σ_e and σ_i are the respective electronic and oxygen ionic conductivity, L the thickness of the membrane [6]. With these in mind, one can conclude that at least for one of the air/He and air/CO gradients, and very probably for both, the overall oxygen permeation process is

Fig. 2 XRD patterns of YSZ–LSC composite. **a** Fresh membrane and **b** inner wall of the membrane tube after exposure to reducing atmosphere at elevated temperatures for 500 h. Δ Denotes $Zr_{0.8}Y_{0.2}O_{1.9}$ and \circ $La_{0.8}Sr_{0.2}CrO_{3-\delta}$



not limited by the transport of oxide ions and electrons in the bulk of the membrane, but by the surface oxygen change. This is because the oxygen permeation processes under the air/He and air/CO gradients involve the same bulk transport process, and if they were all in the bulk-controlled region, there would be no difference in the values of the permeance and activation energy between the two gradients.

Indication of the rate-limiting step also arises from the comparison for YSZ–Pd composite. With composites made of YSZ (60 vol%) and Pd at 950 °C, the oxygen flux scaled to the membrane thickness of 1 mm was $2 \times 10^{-7} \text{ mol cm}^{-2} \text{ s}^{-1}$ under air/CO gradient, and $4 \times 10^{-8} \text{ mol cm}^{-2} \text{ s}^{-1}$ under air/He gradient [5, 11]. These values are 4–5 times larger than those observed for YSZ–LSC membranes under similar conditions. The difference in the measured oxygen permeation flux between the YSZ–Pd and YSZ–LSC composite can be attributed to difference in the surface activity between the Pd and LSC phase. For the dual-phase composites, the surface oxygen exchange, a key step in oxygen permeation, is believed to take place only at the three-phase boundaries (TPB) of gas/oxygen ion conductor/electron conductor. For the YSZ–Pd composite, owing

to the catalytic activity of Pd, the surface process is fast. But for YSZ–LSC composite, the surface process is low because LSC has been known to be inactive toward the surface reaction. As a matter of fact, there are increasing research activities in exploring lanthanum–chromite-based anode material. And it has been shown that doping of LSC phase at B-site with Mn

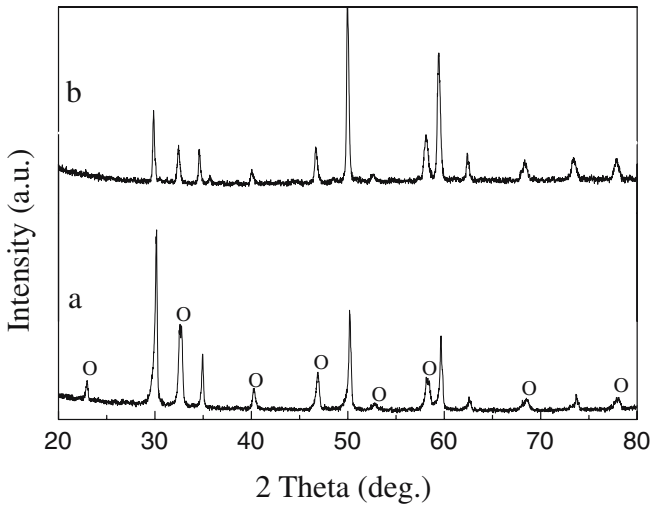


Fig. 3 SEM pictures of YSZ–LSC composite. **a** Fresh membrane and **b** inner wall of the membrane tube after exposure to reducing atmosphere at elevated temperatures for 500 h

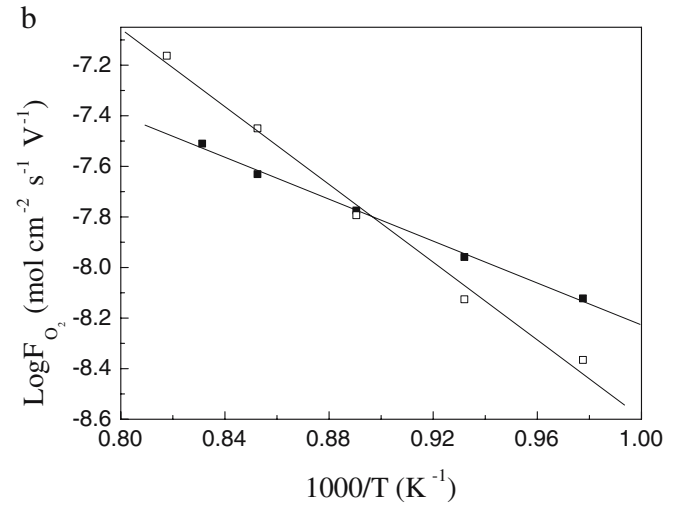
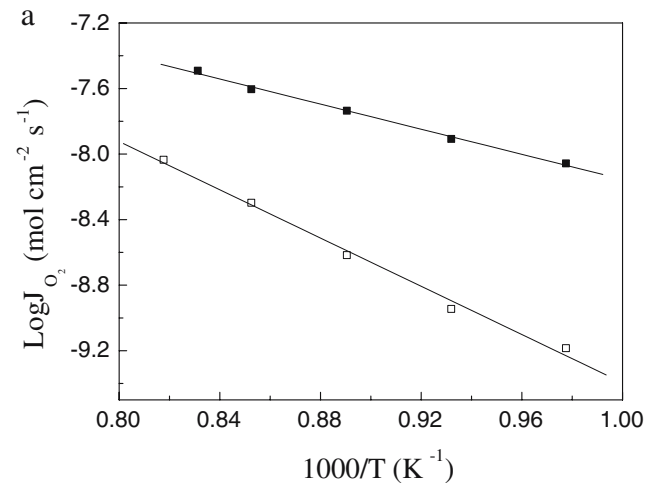


Fig. 4 Arrhenius plot of **a** oxygen permeation and **b** permeance for YSZ–LSC composite. \square Denotes the data obtained under air/helium gradient and \blacksquare the data for air/CO gradient

leads to an improvement in electrochemical activity [12]. One can expect a higher oxygen permeation flux when these doped LSC oxides are used for making composite membrane. The other way of improving the surface oxygen exchange activity is to prepare a nanodispersed composite membrane that should possess a much larger TPB. In principle, these approaches can be applied to improving the surface oxygen exchange activity for YSZ–LSC composite. And as long as the surface process has been promoted to such a degree that it is much faster than the bulk transport, then further increase in oxygen permeation should come from the promotion of the latter. For oxygen permeation flux in proportional to the reciprocal thickness of the membrane in the bulk-controlled region, use of thinner membranes is favorable.

Stability of the membrane

The dual-phase membrane exhibits excellent stability. The membrane tube was found to remain intact after operation for ~500 h at elevated temperature with its inner wall exposed to He, CO, CH₄, and H₂ and outside shell to air. Figure 2b gives the XRD pattern taken from the inner wall of the used membrane tube. It can be seen that the XRD patterns are almost same as those taken before oxygen permeation measurement. Figure 3b presents the SEM picture taken on the inner wall of the used membrane tube. It is shown that the surfaces of the grains have been corroded to some extent, but the grain shape remains unchanged.

Conclusions

The YSZ–LSC composite possesses appreciable oxygen permeability at elevated temperatures, especially under a large oxygen partial pressure gradient. An oxygen permeation as large as 3.2×10^{-8} mol cm⁻² s⁻¹ is obtained under air/CO gradient at 930°C. The YSZ–LSC composite exhibits excellent stability under stringent operation conditions, holding promises for membrane reactor applications.

Acknowledgements This work was supported by National Natural Science Foundation of China (Grant Nos.: 50332040, 50225208) and Anhui Provincial Science Foundation (Grant No. 050440302).

References

1. Teraoka Y, Zhang HM, Furukawa S, Yamazoe N (1985) *Chem Lett* 1743
2. Balatrandran U, Dusek JT, Maiya PS, Ma B, Mievilte RL, Kleefisch MS, Udovich CA (1997) *Catal Today* 36:265
3. Chen CS, Feng SJ, Ran S, Zhu DC, Liu W, Bouwmeester HJM (2003) *Angew Chem Int Ed* 42:5196
4. Mazanec TJ, Cable TL, Frye JG (1992) *Solid State Ion* 53–56:111
5. Chen CS, Kruidhof H, Bouwmeester HJM, Verweij H, Burggraaf AJ (1996) *Solid State Ion* 86–88:569
6. Chen CS, Burggraaf AJ (1999) *J Appl Electrochem* 29:355
7. Kharton VV, Kovalevsky AV, Viskup AP, Figueiredo FM, Yaremchenko AA, Naumovich EN, Marques FMB (2000) *J Electrochem Soc* 147:2814
8. Kim J, Lin YS (2000) *AIChE J* 46–48:1521
9. Chen CS, Zhang ZP, Jiang GS, Fan CG, Liu W, Bouwmeester HJM (2001) *Chem Mater* 13:2797
10. Anderson HU (1992) *Solid State Ion* 52:33
11. Chen CS (1994) Ph.D. Thesis, University of Twente
12. Tao S, Irvine JTS (2003) *Nat Mater* 2:320